Micromorphological Observations of Mira Thin Sections

Paul Goldberg
Boston University

Three 50x75mm thin sections were analyzed from Mira using soil micromorphology (Courty et al., 1989). They were scanned first on a flat-bed scanner in order to reveal overall characteristics of bedding, microstructure, and composition. They were then examined with binocular and petrographic microscopes at magnifications ranging from 8x to 15x (binocular microscope) and from 20x to 200x with the petrographic microscope. Nomenclature follows that of (Courty, Goldberg and Macphail, 1989) and (Stoops, 2003).

Field view of sampling location (courtesy of J. Hoffecker). Visible here are whitish spots and irregular domains, which in thin sections below, are expressed as clean, well-sorted quartz sand with no fine material.

Sample Mira TS 12-1 (3KB1)
This sample – and all samples - overall consists of compact sandy silty clay with fragments of charcoal in the lower quarter of the sample. The charcoal tends to occur as individual, unconnected mm-sized pieces, or as finer, silt sized remains that are well integrated into the matrix, suggesting that it has been incorporated into the matrix by small scale bioturbation (size of earthworms) or weak cryoturbation (see below). Interesting is the presence of localized circular to elongated domains that are comprised of well sorted, clean quartz sand, with no fine

interstitial matrix. Similarly, rounded aggregates of finer silty clay appear to grade into bands of silty clay that at the mesoscale (i.e., ~10x magnification) are reminiscent of ice-lensing features (van Vliet-Lanoe, 1985).

The most interesting aspects of this sample are the presence of charcoal and the sandy domains. The charcoal tends to occur as isolated distinct mm-sized pieces as well as silt-sized charcoal that are well integrated into the finer silty clay matrix. Both occurrences show that the charcoal is not in tact but likely has been reworked biologically or by cold phenomena. The latter is suggested by weak ice lensing in photos below, as well as the capping on an elongated fragment of charcoal. The origin of the sandy domains could similarly related to frost affected soils and appear to be fissures that were later filled with the sand (Van Vliet-Lanoë, 2010). Finally, the generally 'tight' porosity in all samples (although a bit less in this sample which exhibits some vughy porosity) resembles that found in fragic horizons. Again, this observation is consistent with the presence of cold climate conditions.

Macro scan of thin section Mira TS 12-1. The overall massive nature of the sediment is marked here by also the presence of fissures. Note the dark brown pieces and masses of charcoal in the lower fourth of the slide. Arrows point to areas of clean quartz sand. All scans measure 50x75 mm and are in plane-polarized light (PPL).

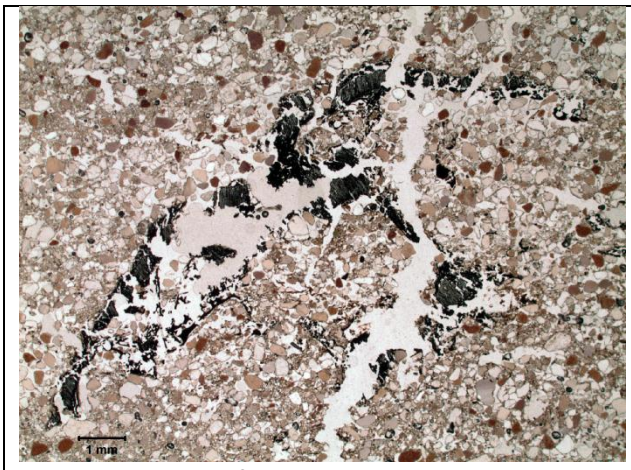

Meso scale view of the charcoal mass shown above. PPL

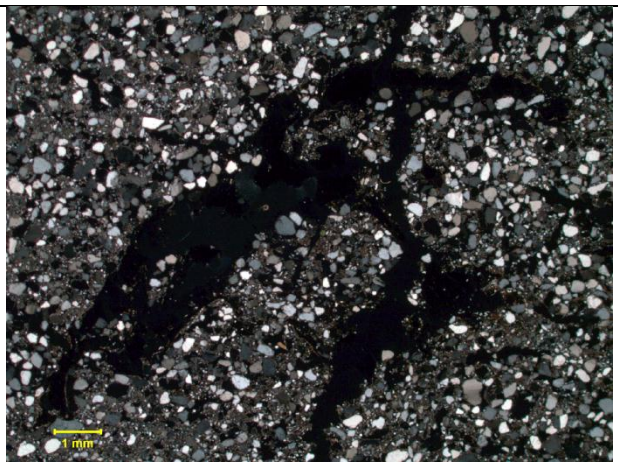

Same as at left but in cross-polarized light (XPL). The sediment is composed of medium sand in at quartz silty clay matrix, shown below.

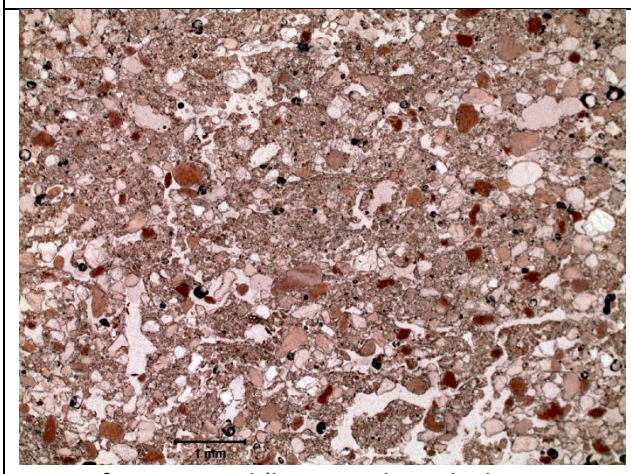

View of quartz sand (brown color, which is an artifact of the photograph) in a silty clay matrix. PPL.

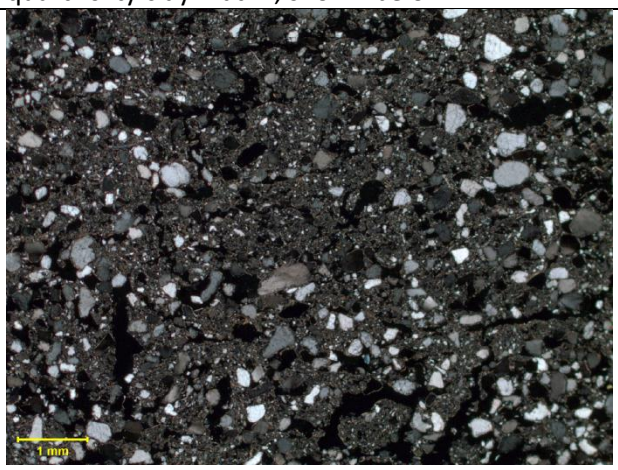

Same as at left but in XPL. Note the vughy porosity here, which is likely produced by roots and some burrowing.

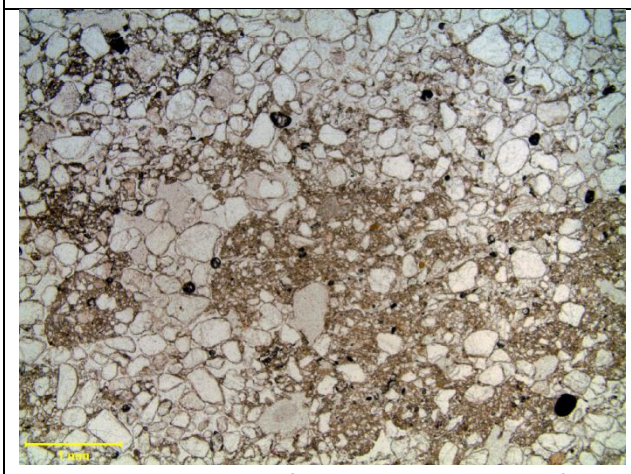

Rounded aggregates of silty clay suggestive of biological reworking by burrowing. Visible at the top are domains of clean quartz sand with little

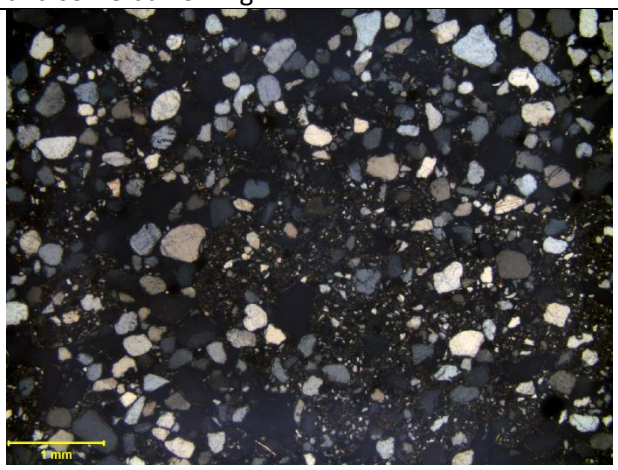

Same as at left but in XPL. The quartz sand domains are more visible here in XPL.

matrix. XPL.

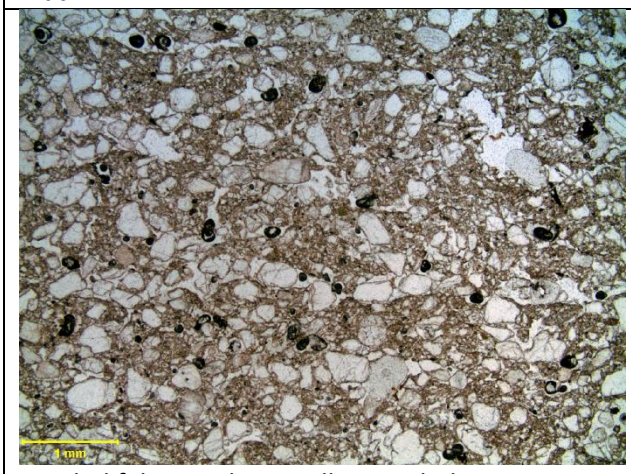

Banded fabric with partially rounded aggregates produced by ice. PPL.

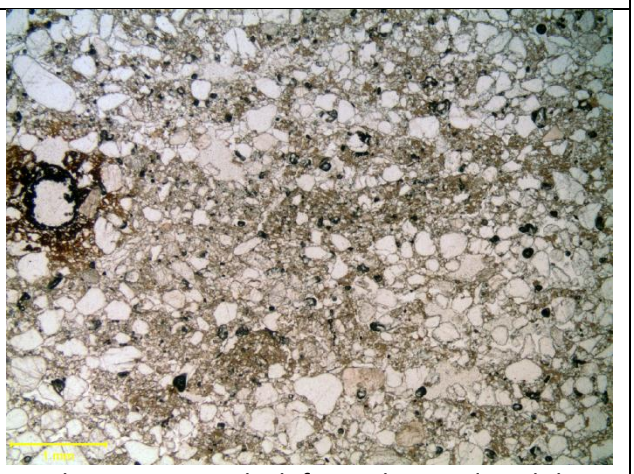

Iron hypocoating, which formed around void that post dates the segregation os the silty lens to the right of it. PPL

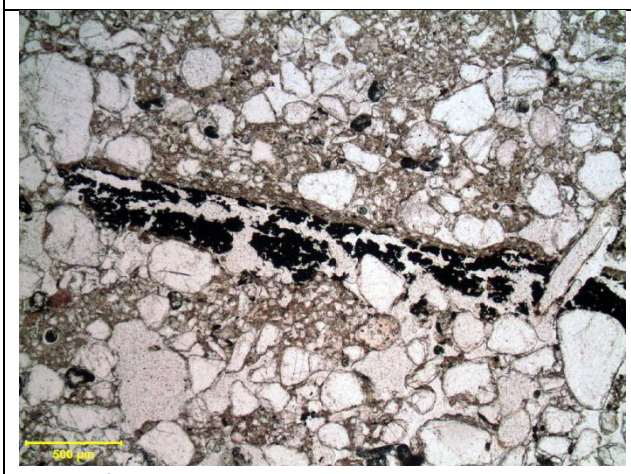

Band of charcoal with silty clay capping, which is also an ice related feature. PPL.

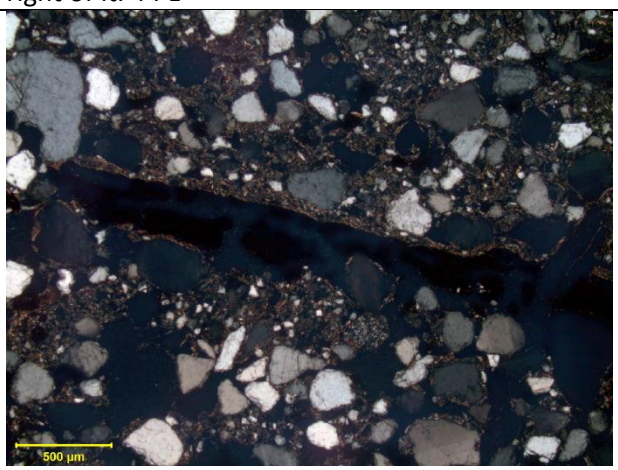

Same as at left but in XPL.

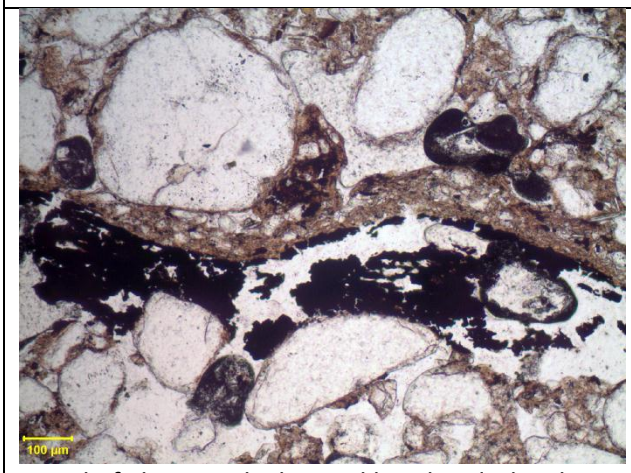

Detail of above with charcoal band and silty clay capping. Cappings are related to freeze-thaw phenomena. PPL.

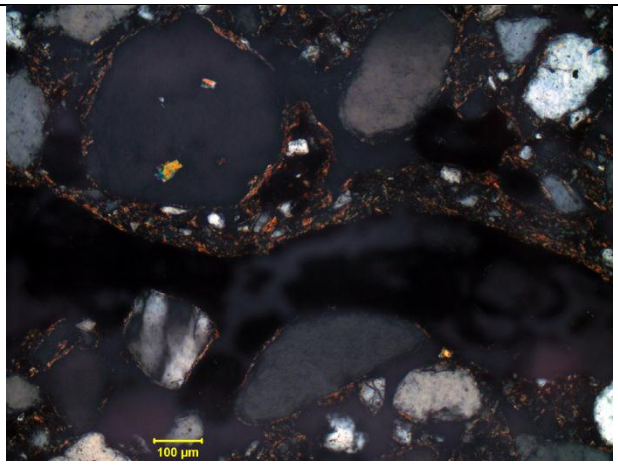

Same as at left but in XPL.

Sample Mira TS 12-2 (3KB2)
This sample, which underlies 12-1, is quite massive and overall richer in the finer silty clay component; the sand grains occur with porphyric related distribution within the matrix, and as above, exhibits mm to cm size domains of clear sand. In addition, mm-size pores display ferruginous hypocoatings, signaling the presence of some gleying/hydromorphism. Along with a greater abundance of fine material, we can also observe some textural pedofeatures. These are expressed ~5 µm thick pale yellow limpid clay coatings around individual sand grains, as well as slightly thicker void coatings formed within the silty clay matrix. This observation is significant as it shows that clay illuviation took place after the suggested freeze-thaw events that produced both the weak banded fabric of the fine fraction and the movement of quartz sand, which as described for sample 12-1 seems to be genetically associated with cold soil phenomena. Unfortunately, it is not possible to determine the horizon from which these clay coatings are derived, only that this horizon overlies that of this sample; it is interesting to note that the overlying sample 12-1 did not contain any translocation features, or any effects of gleying. The fact that the gleying is found also in the underlying sample, 12-3, points to subsurface, groundwater, gleying.

 Macro scan showing massive, compact poorly sorted silty sand with some clay. Note the appearance here of mm-sized circular pores with associated ferruginous hypocoatings. Such massive structure is similar to that found in a fragic horizon.	

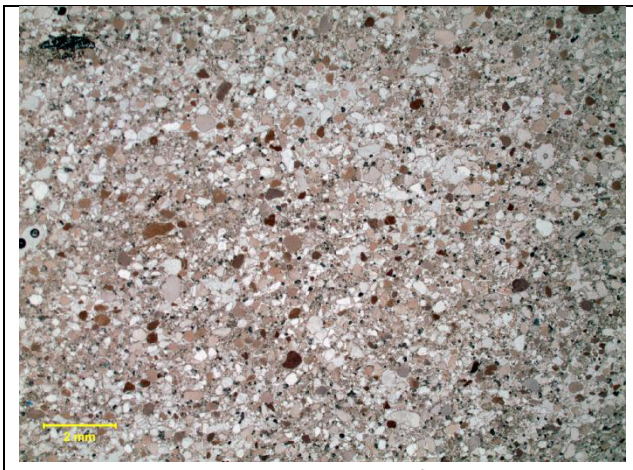

Meso scale view showing detail of compact silty sand matrix. PPL.

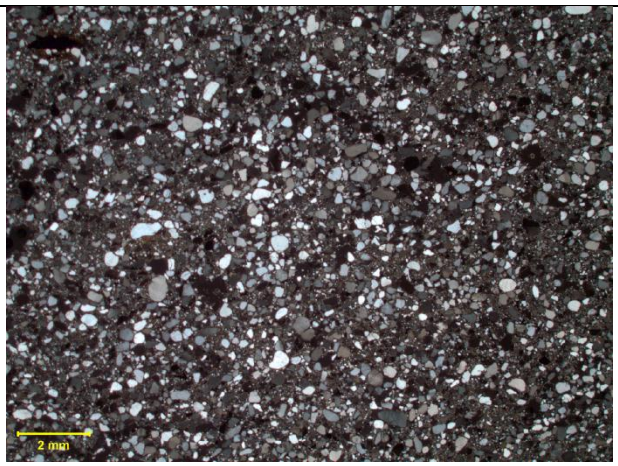

XPL view of image at left. Not the overall lack of porosity.

Grain of iron-stained charcoal in the center (the brownish color of the quartz grains is an artifact of the photograph). PPL.

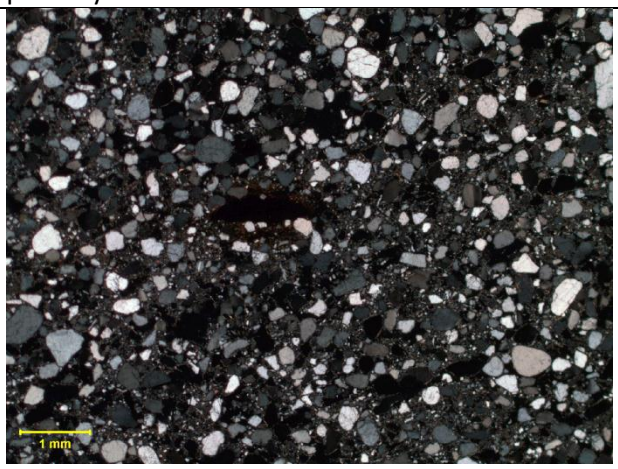

Same as at left but in XPL; porosity is low but expressed by few irregular vughs.

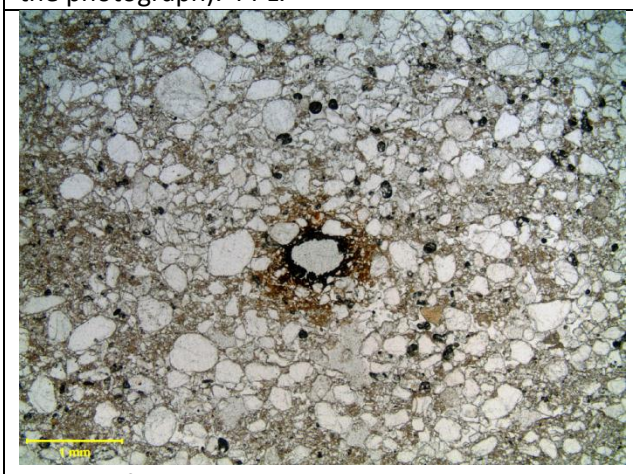

Another ferruginous hypocoating around void formed in a localized domain of sandier sediment. PPL

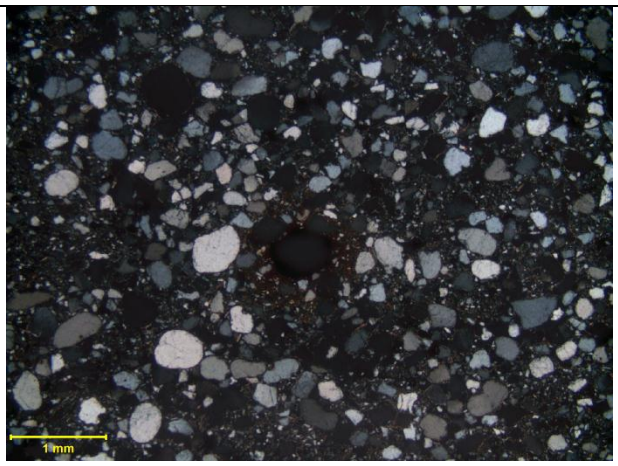

Same as at left but in XPL. The variation in sizes of the quartz from sand to silt sizes is slightly more evident here than in photo at left.

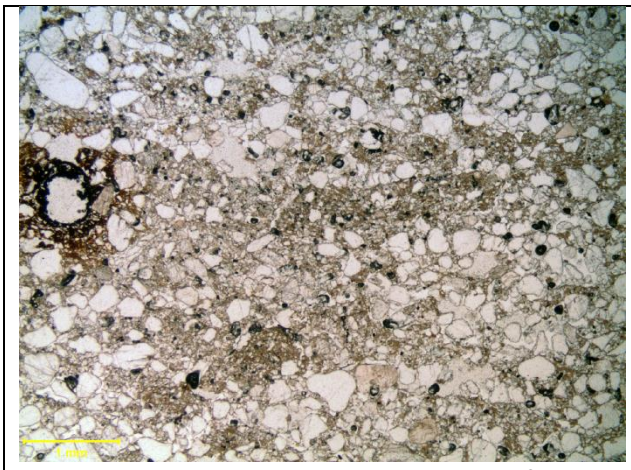

Ferruginous hypocoating around void at left. Note that the void and hypocoating post-date the finer silty clay band in the center. This band appears to be a feature related to freeze-thaw, although such features are not well developed. PPL.

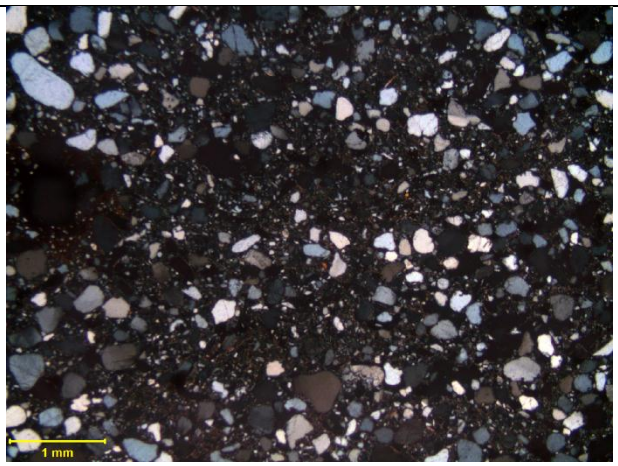

Same as at left but in XPL. The horizontal variation of bands of quartz sand and silty clay can be seen here.

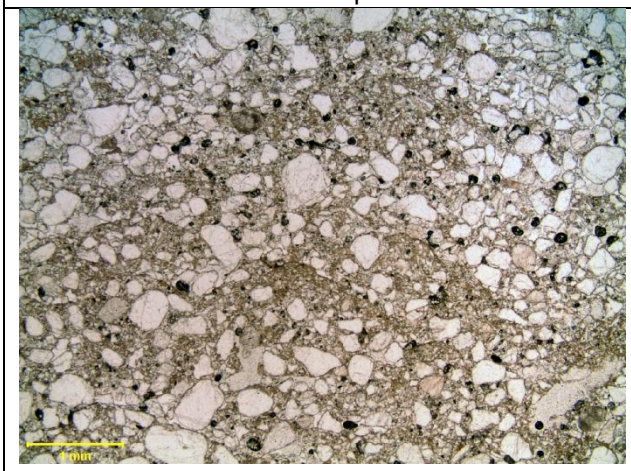

Aggregates and domains of silty clay are mixed with coarser sand; these features are more evident in the XPL view in the photo at right. PPL.

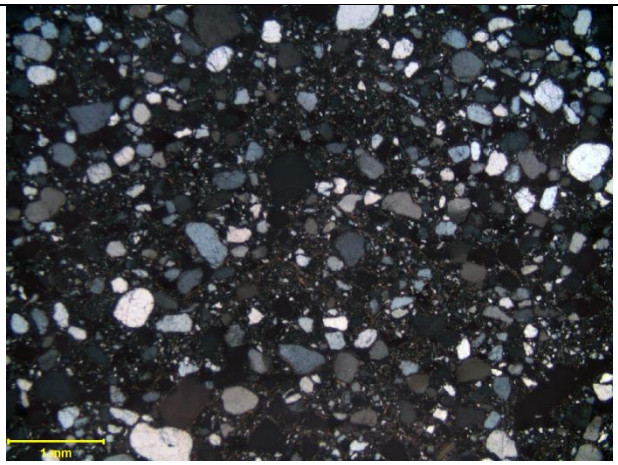

Same as at left but in XPL. The localization of quartz sand can be seen in the photo, particularly in the upper right-hand side.

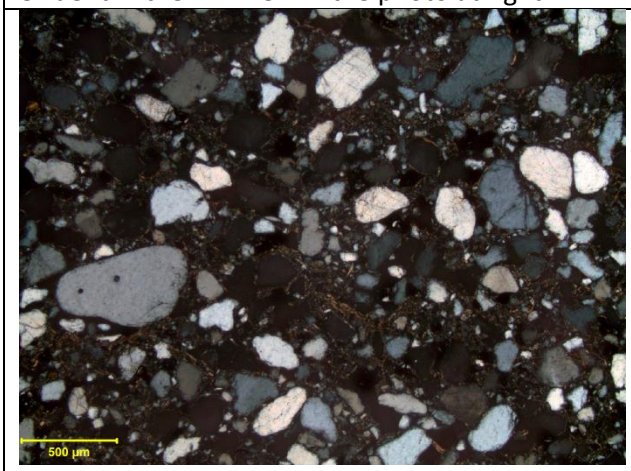

Clayey coatings (brighter reddish brown areas) are

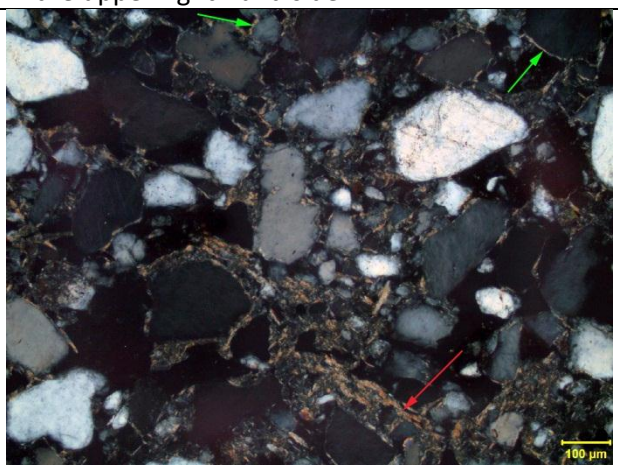

Detail of photo at left showing the clay coatings

concentrated in the lower part of the photograph.	(red arrow), which are more abundant in the lower part; thinner coatings can be seen around individual quartz grains in the upper part (green arrows). The coatings indicate that translocation took place after any textural segregation of the sand and silty clay fractions, which were produced under colder conditions.

Sample Mira TS 12-3 (3KB3)

The proportion of quartz sand to the finer silty clay matrix is similar to that in sample 12-2 above it. On the other hand, the segregation of the quartz fraction from the silty clay matrix is striking in this sample and is displayed by a near vertical, roughly cm-wide tongue of clean quartz sand in the center of the thin section. In addition, secondary iron staining is somewhat less abundant than in sample 12-2, although it is not present as hypocoatings around pores, but as impregnations associated with the remains of charcoal or organic matter. Moreover, translocated clay is more abundant in this sample than in 12-2, and it is somewhat limited to the finer fraction and less so as coatings around coarser quartz grains. This increased degree of translocation suggests that this sample is more within what was a weak Bt horizon. The clearly defined textural tongue containing clean quartz sand, reflects the position of this sample possibly close to a former surface and is part of a number of 'bleached' areas in the field at this position (see field photo above); interestingly, the field photo shows. In any case, it is reasonable that the formation of the tongues is related to frost-affected soils, whereas the translocation of the limpid clay as coatings around quartz grains and void coatings within the matrix is tied to more temperate conditions. The presence of ferruginous impregnations is indicative of groundwater affects that might pre-date the formation of the tongues, as there is no secondary iron staining in the tongues.

 Macro scan showing long tongue of quartz sand crossing the sample vertically. The matrix material is compact and resembles that of other samples.	

Meso scale view of vertical quartz-rich tongue shown above (the brownish color of the quartz grains is an artifact of the photograph). PPL.

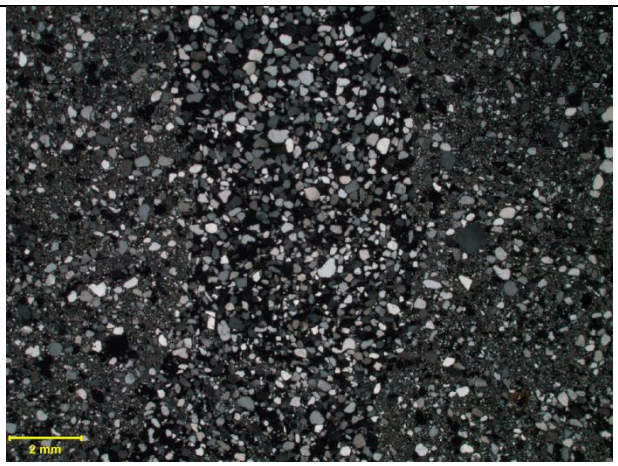

Same as at left but in XPL. Note the loose nature of the well sorted quartz within the tongue.

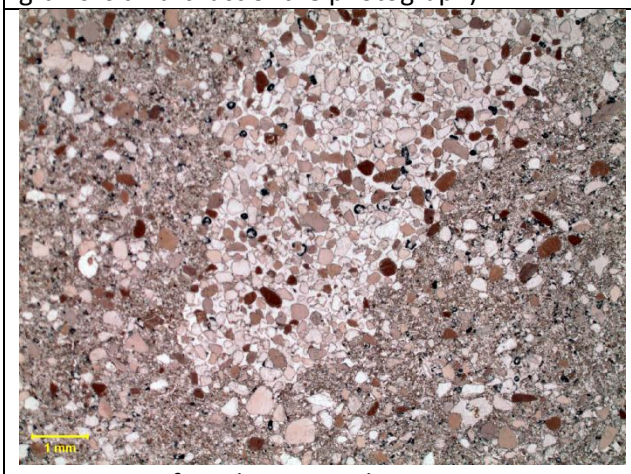

Lower part of sandy tongue shown in macro scan. PPL.

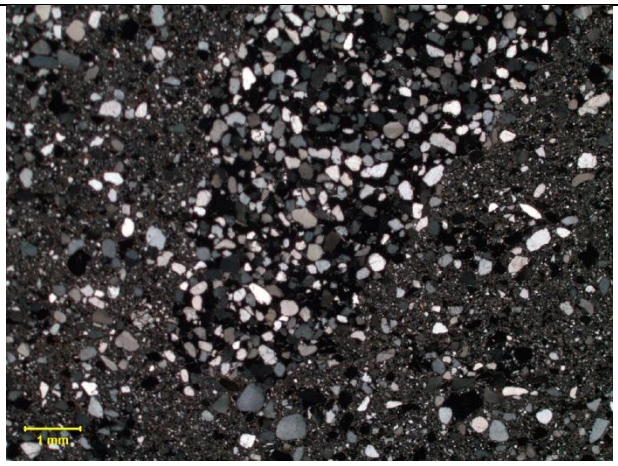

Same as left but in XPL.

Ferruginous impregnation within the silty clay matrix that contains quartz and feldspar sand. XPL.

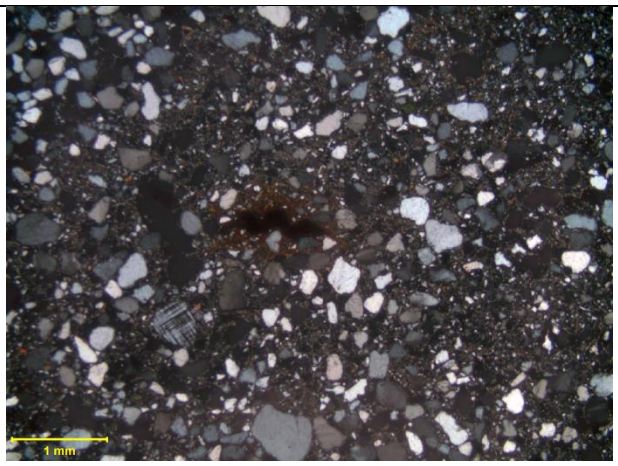

Same as at left but in XPL. Note the twinning in the feldspar grain below and to the left of the iron feature.

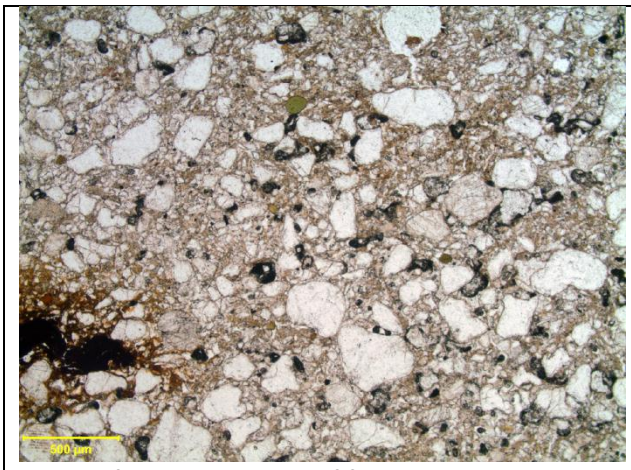

Detail of right-hand part of ferruginous impregnation shown above.

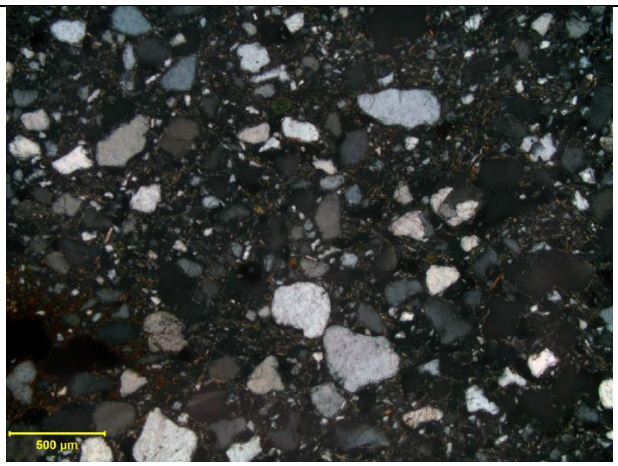

Same as at left but in XPL.

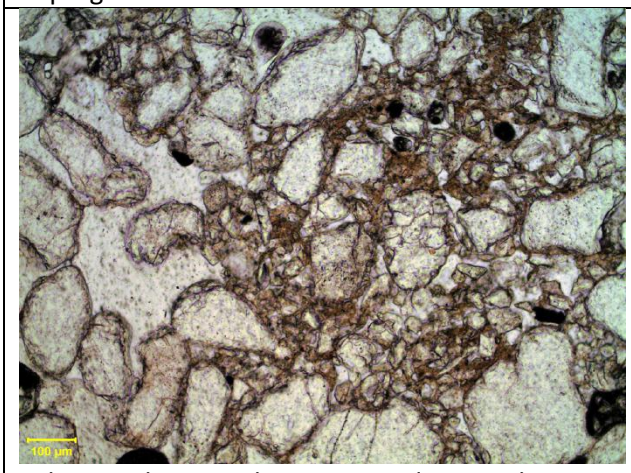

Subvertical contact between sandy, granular quartz within tongue at left, and sandy silty clay matrix at right. XPL.

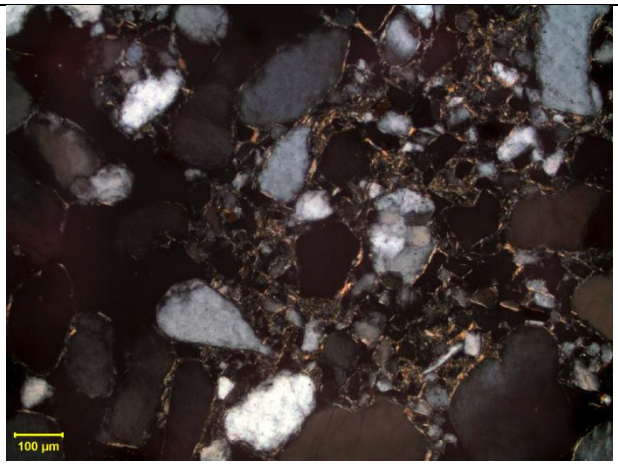

Same as at left but in XPL. Note “clean”, granular nature of the sand at left and the matrix at right, which exhibits reddish orange clay coatings.

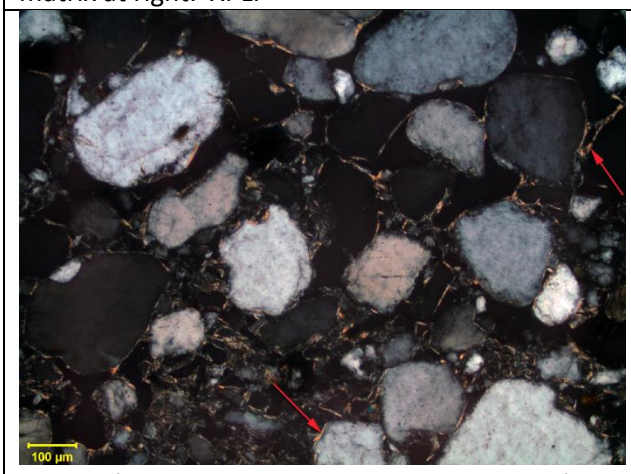

Detail of contact above. Note the presence of clay coatings (arrows) around quartz grains, both those within the tongue at left and upper right, as well as those around grains in finer matrix. This clearly

shows that clay translocation postdates the formation of the sandy tongue. XPL.	

References

Courty, M.-A., Goldberg, P. and Macphail, R.I., 1989. Soils and Micromorphology in Archaeology. Cambridge University Press, Cambridge, 344p.

Stoops, G., 2003. Guidelines for Analysis and Description of Soil and Regolith Thin Sections. Soil Science Society of America, Madison, WI, 184p.

van Vliet-Lanoe, B., 1985. Frost effects in soils. In: J. Boardman (Ed.) Soils and Quaternary Landscape Evolution, pp. 117-158. John Wiley & Sons, Chichester.

Van Vliet-Lanoë, B., 2010. Frost Action. In: G. Stoops, V. Marcelino and F. Mees (Eds.), Interpretation of Micromorphological Features of Soils and Regoliths, pp. 81-108. Elsevier, Amsterdam.